Supporting Information

Photochemical phase transitions enable co-harvesting of photon energy and ambient heat for energetic molecular solar thermal batteries that upgrade thermal energy

Zhao-Yang Zhang,[1] Yixin He,[1] Zhihang Wang,[2] Jiale Xu,[3] Mingchen Xie,[1] Peng Tao,[3] Deyang Ji,[4] Kasper Moth-Poulsen,[2,*] and Tao Li[1,*]

[1]School of Chemistry and Chemical Engineering, Frontiers Science Center for Transformative Molecules, Shanghai Key Laboratory of Electrical Insulation and Thermal Aging, Key Laboratory of Thin Film and Microfabrication (Ministry of Education), Shanghai Jiao Tong University, Shanghai, 200240, China. E-mail: litao1983@sjtu.edu.cn

[2]Department of Chemistry and Chemical Engineering, Chalmers University of Technology, 41296 Gothenburg, Sweden. E-mail: kasper.moth-poulsen@chalmers.se

[3]State Key Laboratory of Metal Matrix Composites, School of Materials Science and Engineering, Shanghai Jiao Tong University, Shanghai, 200240, China.

[4]Institute of Molecular Aggregation Science, Tianjin University, Tianjin, 300072 China.

Table of contents

Synthesis

Azo compounds **A1-A12**, **B3**, **B7** and **B11** were reported in our previous work.[1] **B4-B6**, **B8-B10** were prepared using the same procedure. They were purified by column chromatography and recrystallization. NMR and HRMS data of these compounds are reported in the following.

B4 (**pzAzo ether 4ene**)

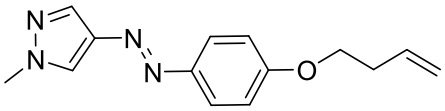

^{1}H NMR (400 MHz, Chloroform-*d*): δ 7.98 (s, 1H, -N=C***H***-, pyrazol), 7.91 (s, 1H, -N-C***H***=, pyrazol), 7.77 (d, *J* = 8.9 Hz, 2H, =N-C(-C***H***=)(=C***H***-), benzene), 6.97 (d, *J* = 8.9 Hz, 2H, -O-C(-C***H***=)(=C***H***-), benzene), 5.92 (ddt, *J* = 17.0, 10.3, 6.7 Hz, 1H, -C***H***=CH_2), 5.16 (dd, *J* = 24.0, 13.7 Hz, 2H, -CH=C***H$_2$***), 4.08 (t, *J* = 6.7 Hz, 2H, -O-C***H$_2$***-), 3.96 (s, 3H, -N-C***H$_3$***), 2.57 (q, *J* = 6.7 Hz, 2H, -O-CH_2-C***H$_2$***-); **^{13}C NMR** (101 MHz, Chloroform-*d*): δ 160.92 (-O-***C***, benzene), 147.28 (=N-***C***, benzene), 142.01 (4'***C***, pyrazol), 134.33 (-***C***H=CH_2), 133.38 (3'***C***, pyrazol), 126.29 (5'***C***, pyrazol), 124.05 (=N-C(-***C***H=)(=***C***H-), benzene), 117.38 (-CH=***C***H_2), 114.86 (-O-C(-***C***H=)(=***C***H-), benzene), 67.60 (-O-***C***H_2-), 39.69 (-N-***C***H_3), 33.70 (-O-CH_2-***C***H_2-); **HRMS** (ESI): m/z calculated for $[C_{14}H_{16}N_4OH]^+$ 256.1397, found 256.1396.

B5 (**pzAzo ether 5ene**)

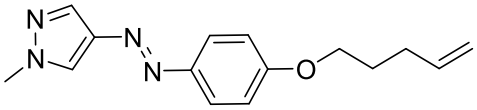

^{1}H NMR (400 MHz, Chloroform-*d*): δ 7.98 (s, 1H, -N=C***H***-, pyrazol), 7.91 (s, 1H, -N-C***H***=, pyrazol), 7.77 (d, *J* = 9.0 Hz, 2H, =N-C(-C***H***=)(=C***H***-), benzene), 6.97 (d, *J* = 9.0 Hz, 2H, -O-C(-C***H***=)(=C***H***-), benzene), 5.86 (ddt, *J* = 16.9, 10.2, 6.6 Hz, 1H, -C***H***=CH_2), 5.05 (dd, *J* = 26.0, 15.5 Hz, 2H, -CH=C***H$_2$***), 4.04 (t, *J* = 6.4 Hz, 2H, -O-C***H$_2$***-), 3.96 (s, 3H, -N-C***H$_3$***), 2.26 (q, *J* = 7.3 Hz, 2H, -C***H$_2$***-CH=CH_2), 1.92 (p, *J* = 6.6 Hz, 2H, -O-CH_2-C***H$_2$***-); **^{13}C NMR** (101 MHz, Chloroform-*d*): δ 161.11 (-O-***C***, benzene), 147.21 (=N-***C***, benzene), 142.03 (4'***C***, pyrazol), 137.81 (-***C***H=CH_2), 133.38 (3'***C***, pyrazol), 126.28 (5'***C***, pyrazol), 124.05 (=N-C(-***C***H=)(=***C***H-), benzene), 115.47 (-CH=***C***H_2), 114.82 (-O-C(-***C***H=)(=***C***H-), benzene), 67.59 (-O-***C***H_2-), 39.69 (-N-***C***H_3), 30.20 (-O-$(CH_2)_2$-***C***H_2-), 28.49 (-O-CH_2-***C***H_2-); **HRMS** (ESI): m/z calculated for $[C_{15}H_{18}N_4OH]^+$ 270.1553, found 270.1551.

B6 (**pzAzo ether 6ene**)

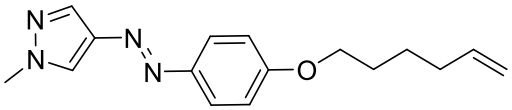

^{1}H NMR (400 MHz, Chloroform-*d*): δ 7.98 (s, 1H, -N=C***H***-, pyrazol), 7.91 (s, 1H, -N-C***H***=, pyrazol), 7.77 (d, *J* = 8.9 Hz, 2H, =N-C(-C***H***=)(=C***H***-), benzene), 6.96 (d, *J* = 8.9 Hz, 2H, -O-C(-C***H***=)(=C***H***-), benzene), 5.83 (ddt, *J* = 16.9, 10.2, 6.7 Hz, 1H, -C***H***=CH_2), 5.01 (dd, *J* = 23.7, 13.7 Hz, 2H, -CH=C***H$_2$***), 4.02 (t, *J* = 6.4 Hz, 2H, -O-C***H$_2$***-), 3.95 (s, 3H, -N-C***H$_3$***), 2.14 (q, *J* = 7.1 Hz, 2H, -C***H$_2$***-CH=CH_2), 1.83 (p, *J* = 7.0 Hz, 2H, -O-CH_2-C***H$_2$***-), 1.59 (p, *J* = 7.5 Hz, 2H, -O-$(CH_2)_2$-(C***H$_2$***)$_3$-); **^{13}C NMR** (101 MHz, Chloroform-*d*): δ 161.13 (-O-***C***, benzene), 147.16 (=N-***C***, benzene), 142.01 (4'***C***, pyrazol), 138.57 (-***C***H=CH_2), 133.36 (3'***C***, pyrazol), 126.26 (5'***C***, pyrazol), 124.04 (=N-C(-***C***H=)(=***C***H-), benzene), 114.95 (-O-C(-***C***H=)(=***C***H-), benzene), 114.78 (-CH=***C***H_2), 68.19 (-O-***C***H_2-), 39.68 (-N-***C***H_3), 33.53 (-O-$(CH_2)_3$-***C***H_2-), 28.76 (-O-CH_2-***C***H_2-), 25.41 (-O-$(CH_2)_2$-***C***H_2-); **HRMS** (ESI): m/z calculated for $[C_{16}H_{20}N_4OH]^+$ 285.1710, found 285.1709.

B8 (**pzAzo ether 8ene**)

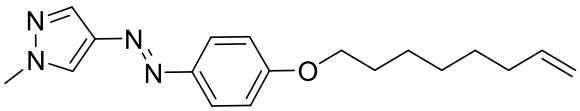

^{1}H NMR (400 MHz, Chloroform-*d*): δ 7.98 (s, 1H, -N=C***H***-, pyrazol), 7.90 (s, 1H, -N-C***H***=, pyrazol), 7.77 (d, *J* = 8.9 Hz, 2H, =N-C(-C***H***=)(=C***H***-), benzene), 6.96 (d, *J* = 8.9 Hz, 2H, -O-C(-C***H***=)(=C***H***-), benzene), 5.82 (ddt, *J* = 16.9, 10.2, 6.7 Hz, 1H, -C***H***=CH_2), 4.97 (dd, *J* = 24.3, 13.6 Hz, 2H, -CH=C***H$_2$***), 4.01 (t, *J* = 6.5 Hz, 2H, -O-C***H$_2$***-), 3.95 (s, 3H, -N-C***H$_3$***), 2.07 (q, *J* = 6.6 Hz, 2H, -C***H$_2$***-CH=CH_2), 1.81 (p, *J* = 6.7 Hz, 2H, -O-CH_2-C***H$_2$***-), 1.52 – 1.37 (m, 6H, -O-$(CH_2)_2$-(C***H$_2$***)$_3$-); **^{13}C NMR** (101 MHz, Chloroform-*d*): δ 161.18 (-O-***C***, benzene), 147.13 (=N-***C***, benzene), 142.01 (4'***C***, pyrazol), 139.11 (-***C***H=CH_2), 133.35 (3'***C***, pyrazol), 126.25 (5'***C***, pyrazol), 124.03 (=N-C(-***C***H=)(=***C***H-), benzene), 114.78 (-O-C(-***C***H=)(=***C***H-), benzene), 114.45 (-CH=***C***H_2), 68.37 (-O-***C***H_2-), 39.67 (-N-***C***H_3), 33.81 (-O-$(CH_2)_6$-***C***H_2-), 29.27 (-O-CH_2-***C***H_2-), 28.95 (-O-$(CH_2)_3$-***C***H_2-), 28.93 (-O-$(CH_2)_4$-***C***H_2-), 25.99 (-O-$(CH_2)_2$-***C***H_2-); **HRMS** (ESI): m/z calculated for $[C_{18}H_{24}N_4OH]^+$ 313.2022, found 313.2023.

B9 (**pzAzo ether 9ene**)

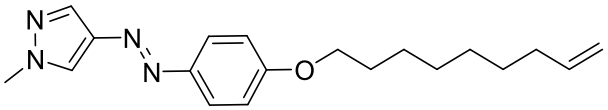

^{1}H NMR (400 MHz, Chloroform-*d*): δ 7.98 (s, 1H, -N=C***H***-, pyrazol), 7.89 (s, 1H, -N-C***H***=, pyrazol), 7.77 (d, *J* = 8.8 Hz, 2H, =N-C(-C***H***=)(=C***H***-), benzene), 6.95 (d, *J* = 8.8 Hz, 2H, -O-C(-C***H***=)(=C***H***-), benzene), 5.81 (ddt, *J* = 16.9, 10.2, 6.7 Hz, 1H, -C***H***=CH$_2$), 4.97 (dd, *J* = 24.1, 13.6 Hz, 2H, -CH=C***H$_2$***), 4.00 (t, *J* = 6.5 Hz, 2H, -O-C***H$_2$***-), 3.93 (s, 3H, -N-C***H$_3$***), 2.05 (q, *J* = 6.7 Hz, 2H, -C***H$_2$***-CH=CH$_2$), 1.79 (p, *J* = 6.7 Hz, 2H, -O-CH$_2$-C***H$_2$***-), 1.50 – 1.31 (m, 8H, -O-(CH$_2$)$_2$-(C***H$_2$***)$_4$-); **^{13}C NMR** (101 MHz, Chloroform-*d*): δ 161.15 (-O-***C***, benzene), 147.09 (=N-***C***, benzene), 141.97 (4'***C***, pyrazol), 139.17 (-***C***H=CH$_2$), 133.29 (3'***C***, pyrazol), 126.22 (5'***C***, pyrazol), 124.00 (=N-C(-***C***H=)(=***C***H-), benzene), 114.74 (-O-C(-***C***H=)(=***C***H-), benzene), 114.33 (-CH=***C***H$_2$), 68.35 (-O-***C***H$_2$-), 39.62 (-N-***C***H$_3$), 33.85 (-O-(CH$_2$)$_6$-***C***H$_2$-), 29.30 (-O-CH$_2$-***C***H$_2$-), 29.27 (-O-(CH$_2$)$_3$-***C***H$_2$-), 29.10 (-O-(CH$_2$)$_4$-***C***H$_2$-), 28.92 (-O-(CH$_2$)$_5$-***C***H$_2$-), 26.05 (-O-(CH$_2$)$_2$-***C***H$_2$-); **HRMS** (ESI): m/z calculated for [C$_{19}$H$_{26}$N$_4$OH]$^+$ 327.2179, found 327.2183.

B10 (**pzAzo ether 10ene**)

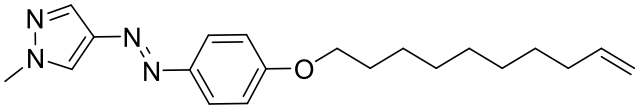

^{1}H NMR (400 MHz, Chloroform-*d*): δ 7.98 (s, 1H, -N=C***H***-, pyrazol), 7.91 (s, 1H, -N-C***H***=, pyrazol), 7.77 (d, *J* = 8.9 Hz, 2H, =N-C(-C***H***=)(=C***H***-), benzene), 6.96 (d, *J* = 8.9 Hz, 2H, -O-C(-C***H***=)(=C***H***-), benzene), 5.82 (ddt, *J* = 16.9, 10.2, 6.7 Hz, 1H, -C***H***=CH$_2$), 4.96 (dd, *J* = 24.5, 13.6 Hz, 2H, -CH=C***H$_2$***), 4.01 (t, *J* = 6.5 Hz, 2H, -O-C***H$_2$***-), 3.96 (s, 3H, -N-C***H$_3$***), 2.05 (q, *J* = 6.7 Hz, 2H, -C***H$_2$***-CH=CH$_2$), 1.80 (p, *J* = 6.7 Hz, 2H, -O-CH$_2$-C***H$_2$***-), 1.51 – 1.30 (m, 10H, -O-(CH$_2$)$_2$-(C***H$_2$***)$_4$-); ^{13}C NMR (101 MHz, Chloroform-*d*): δ 161.12 (-O-***C***, benzene), 147.05 (=N-***C***, benzene), 141.93 (4'***C***, pyrazol), 139.22 (-***C***H=CH$_2$), 133.29 (3'***C***, pyrazol), 126.15 (5'***C***, pyrazol), 123.95 (=N-C(-***C***H=)(=***C***H-), benzene), 114.70 (-O-C(-***C***H=)(=***C***H-), benzene), 114.21(-CH=***C***H$_2$), 68.34 (-O-***C***H$_2$-), 39.60 (-N-***C***H$_3$), 33.83 (-O-(CH$_2$)$_7$-***C***H$_2$-), 29.43(-O-(CH$_2$)$_3$-***C***H$_2$-), 29.36 (-O-CH$_2$-***C***H$_2$-), 29.24 (-O-(CH$_2$)$_6$-***C***H$_2$-), 29.09 (-O-(CH$_2$)$_5$-***C***H$_2$-), 28.94 (-O-(CH$_2$)$_4$-***C***H$_2$-), 26.04 (-O-(CH$_2$)$_2$-***C***H$_2$-); HRMS (ESI): m/z calculated for [C$_{20}$H$_{28}$N$_4$OH]$^+$ 341.2336, found 341.2338.

Instruments and characterization

1. Light irradiations

A 365 nm LED lamp (120 mW/cm^2, light spot diameter of 2 cm) and a 532 nm laser (110 mW/cm^2, beam diameter of 1.3 cm) were used throughout the experiments for charging and discharging.

2. Instrumental characterization

UV-Vis absorption spectra were recorded on UV-2700 spectrophotometer (Shimadzu). Optical microscopic photographs/videos were acquired using a BX3M-ILH microscope (Olympus). XRD patterns were measured on a Bruker D8 Advance diffractometer. ^{1}H NMR spectra were obtained on AVANCE III HD 400 spectrometers (Bruker) with chemical shift of the residual solvent as an internal reference. DSC curves were scanned on a 204 F1 calorimeter (Netzsch) at a heating rate of 10 ^{o}C/min under N_2 atmosphere. IR thermal images/videos were acquired by a T620 thermal IR camera (FLIR). TGA was performed on a STA 449F3 thermal analyser (Netzsch) at a heating rate of 10 ^{o}C/min under N_2 atmosphere.

Quantum yield and solar energy conversion efficiency

Photoisomerization quantum yield (ϕ) was measured by using an established method from literature.[2] Solutions in acetonitrile with absorbance at 365 nm roughly above 2.0 were prepared for each measurement. The concentration was calculated by taking an absorption wavelength close to the maximum of the spectrum at 384 nm, 378 nm, 387 nm and 389 nm for compounds **A1**, **A6**, **B6** and **B8**, respectively.

The solar energy conversion efficiency (η) can be estimated with equation (1) under AM 1.5 solar irradiation spectrum:[3]

$$\eta = \frac{\int_0^{\lambda_{\text{onset}}} \frac{E_{\text{AM 1.5}}(\lambda) \cdot \phi \cdot \Delta H_{\text{isom}}}{h\nu \cdot N_{\text{A}}} \cdot d\lambda}{\int E_{\text{AM 1.5}}(\lambda) \cdot d\lambda} \cdot 100\ \% \qquad (1)$$

where $E_{\text{AM 1.5}}(\lambda)$ corresponds to the AM 1.5 solar spectral irradiance in J s^{-1} m^{-2} nm^{-1}; h is the Plank constant in J s; ν is to the frequency of incoming light in s^{-1}, and N_{A} stands for Avogadro's constant.

Table S1. Quantum yield results for *trans*→*cis* photoisomerization of typical **pzAzo ethers**

365 nm LED Photon flux: 2.88×10^{-8} mol s^{-1}		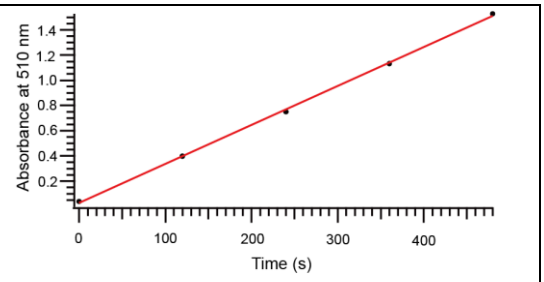
A1 **@384 nm** ϕ_1 = 40.75% ϕ_2 = 41.94% $\phi_{average}$ = 41.35 ±0.60%	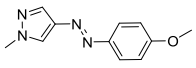	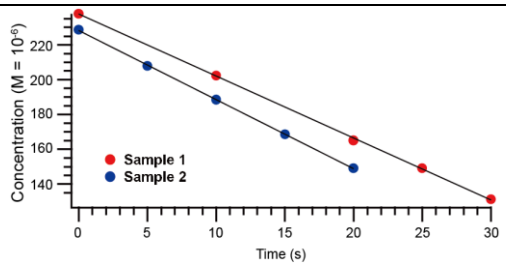
A6 **@378 nm** ϕ_1 = 44.00% ϕ_2 = 44.40% $\phi_{average}$ = 44.2 ±0.20%	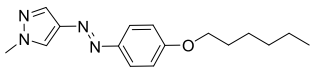	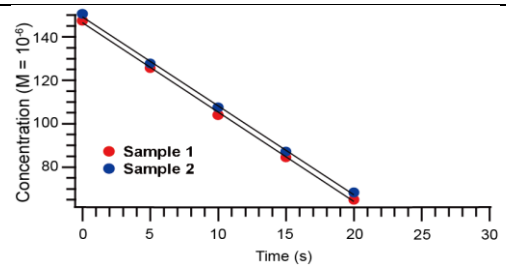
B6 **@387 nm** ϕ_1 = 42.24% ϕ_2 = 41.70% $\phi_{average}$ = 41.97 ±0.27%	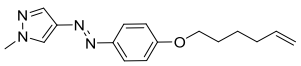	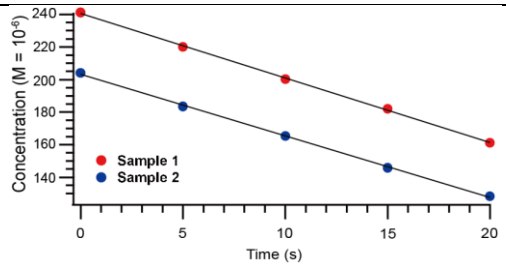
B8 **@389 nm** ϕ_1 = 41.16% ϕ_2 = 39.87% $\phi_{average}$ = 40.52 ±0.65%	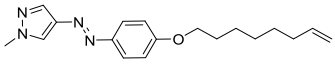	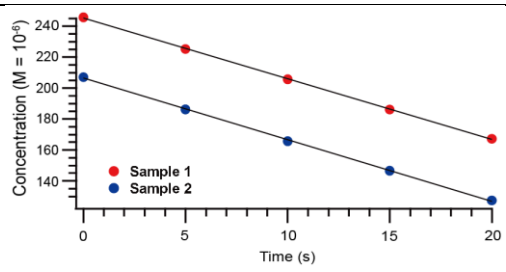

Table S2. Properties of typical **pzAzo ethers**

Molecules	ΔH_{isom} (kJ mol^{-1})	$\phi_{trans\text{-}cis}$	λ_{onset} (nm) (ε>100)	η
A1 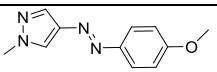 Molecular Weight: 216.24	48.7[a] 51.5[b]	41.35 ± 0.60%	487	1.18%
A6 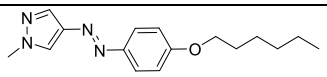 Molecular Weight: 286.38	51.0[a]	44.2 ± 0.20%	484	1.28%
B6 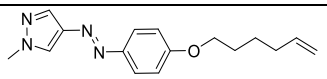 Molecular Weight: 284.36	52.9[a]	41.97 ± 0.27%	484	1.26%
B8 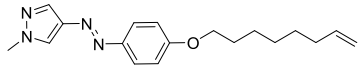 Molecular Weight: 312.42	52.5[a]	40.52 ± 0.65%	484	1.21%

[a] Data determined by DSC.

[b] Data calculated by DFT at the PBE0-D3/6-31G** level of theory in gas phase[1].

Table S3. A list of solar energy conversion efficiencies of azo materials for energy storage reported in literature.

Azo-materials	η	Reference
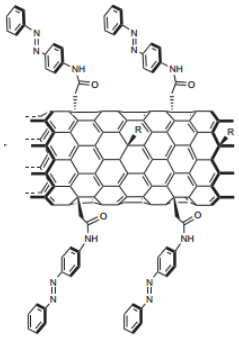	0.3%	4
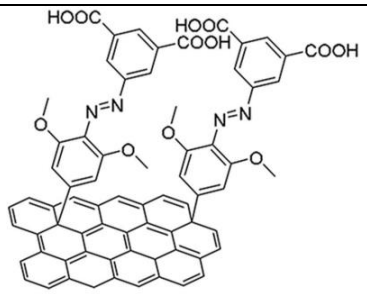	0.27%	5
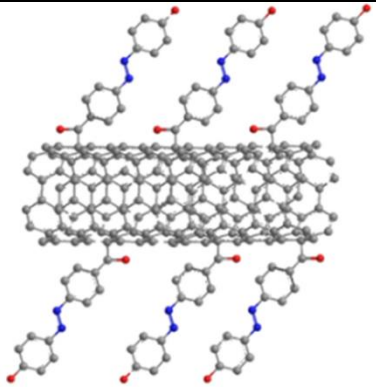	0.25%	6
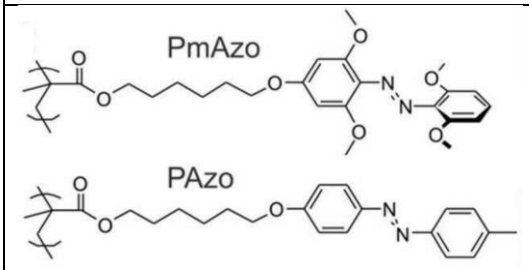	0.4%	7
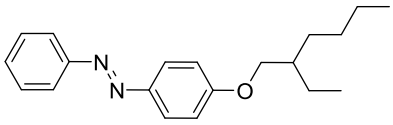	0.88%	8

Thermophysical and thermochemical properties

Table S4. Thermal properties of **An** in *trans* and *cis* states.

An	*trans*				*cis*		*trans* from *cis*-liquid→*trans*-liquid conversion
n	T_m (°C)	T_{cryst} (°C)	ΔH_m (J/g)	ΔH_{cryst} (J/g)	T_m (°C)	ΔH_{isom} (J/g)	ΔH_{cryst} (J/g)
1	113.1	87.4	160.4	142.2	71.2	225.1	126.6
2[a]	110.4	91.0	136.5	127.8	78.2	-	-
3	105.5	76.3	156.8	139.2	89.1	213.1	147.2
4[a]	101.2	74.4	149.7	136.6	54.5	-	-
5[a]	95.6	69.7	171.2	153.2	44.9	-	-
6[a]	93.4	77.6	167.1	162.1	27.0	175.7	154.0
7	96.8	80.4	183.3	182.3	41.2	173.8	180.4
8	95.9	85.8	192.7	204.2	42.5	167.8	192.5
9	101.0	88.2	214.3	211.3	49.6	176.5	226.4
10	99.6	82.2	200.8	200.6	55.9	-	-
11	104.6	91.7	239.7	237.6	59.4	156.7	226.5
12	102.1	92.8	226.1	224.8	64.0	151.9	224.3

[a] Two melting/crystallization peaks were found in DSC curves; T_m/T_{cryst} reported here corresponded to the major peak, and ΔH_m/ΔH_{cryst} reported here was the total value of the two peaks.

Table S5. Thermal properties of **Bn** in *trans* and *cis* states

Bn	*trans*				*cis*		*trans* from *cis*-liquid→*trans*-liquid conversion
n	T_m (°C)	T_{cryst} (°C)	ΔH_m (J/g)	ΔH_{cryst} (J/g)	T_m (°C)	ΔH_{isom} (J/g)	ΔH_{cryst} (J/g)
3	102.6	89.2	140.6	132.5	65.2	223.3	133.3
4[a]	86.4	72.6	143.9	129.6	63.4	-	-
5	90.0	73.6	140.8	140.6	46.6	209.9	140.7
6[a]	82.5	73.0	155.3	148.7	24.8	186.8	139.1
7	83.0	65.9	169.9	163.5	34.8	180.4	156.0
8	82.8	59.7	174.9	170.4	19[b]	167.8	160.8
9	87.1	71.2	180.2	183.6	49.8	-	-
10	88.2	72.6	191.1	189.3	27.5	164.2	184.9
11	91.8	75.2	208.3	208.5	37.3	162.7	205.2

[a] Two melting/crystallization peaks were found in DSC curves; T_m/T_{cryst} reported here corresponded to the major peak, and ΔH_m/ΔH_{cryst} reported here was the total value of the two peaks.

[b] Measured by the Thiele tube method.

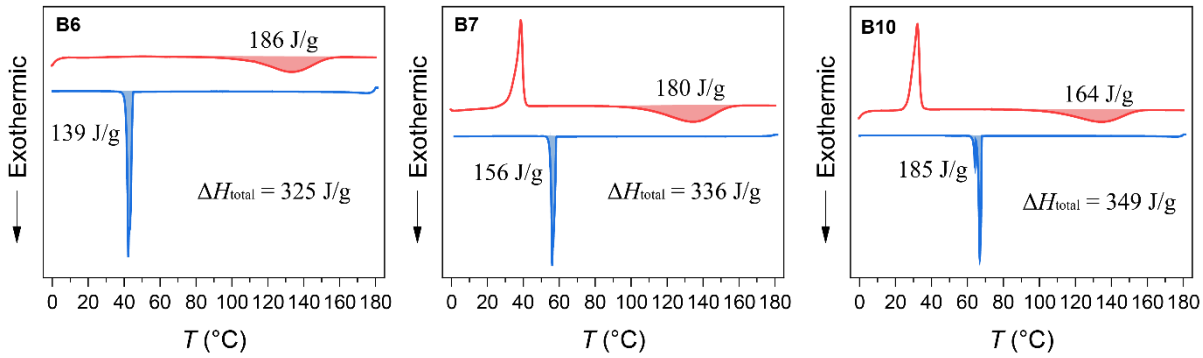

Figure S1. DSC curves of *cis* **B6**, **B7**, and **B10** measured at 10 °C/min (heating and cooling curves are not shown to the same scale of Y-axis for clarity). For **B7** and **B10**, an endothermic peak appeared first in heating curves, as a result of the melting of the crystalline *cis* state. In case of **B6**, melting process was not observed because the *cis* sample was already melted when loaded into the crucibles.

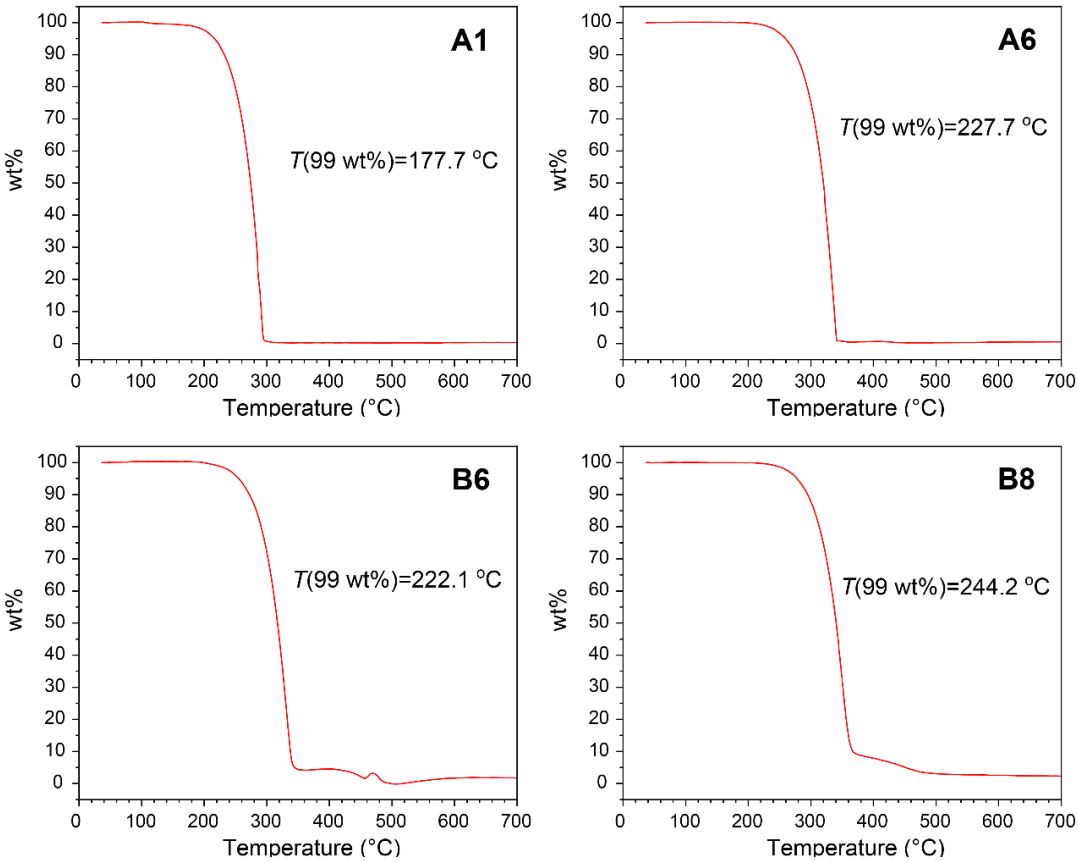

Figure S2. TGA curves of representative azo compounds (20 °C/min, N_2 atmosphere). *T*(99 wt%) refer to the temperature at 1.0 % weight loss.

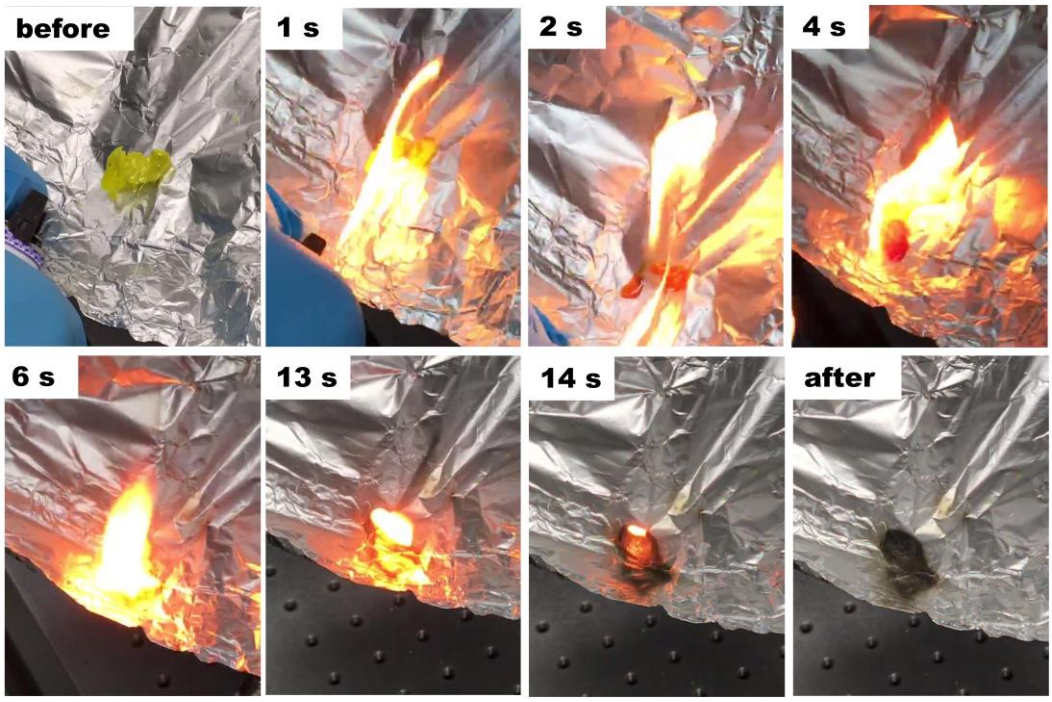

Figure S3. Flammability test. To do this test, a piece of trans-crystal material on aluminum foil was ignited using a lighter. One could see that the sample melted into liquids and burst into flames quickly. The burning lasted for ~12 seconds and left some ashes in the end.

Photo-discharging of *cis*-B8 droplet

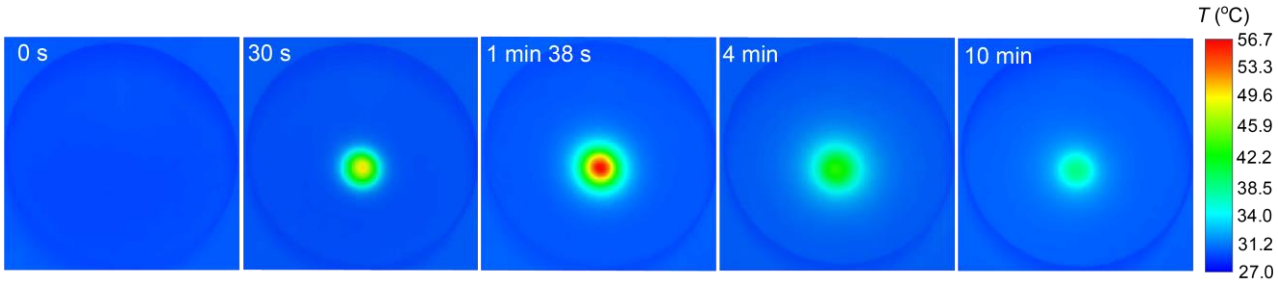

Figure S4. Representative IR thermal images during photo-discharging of a *cis*-**B8** droplet.

Fabrication of *cis*-liquid films

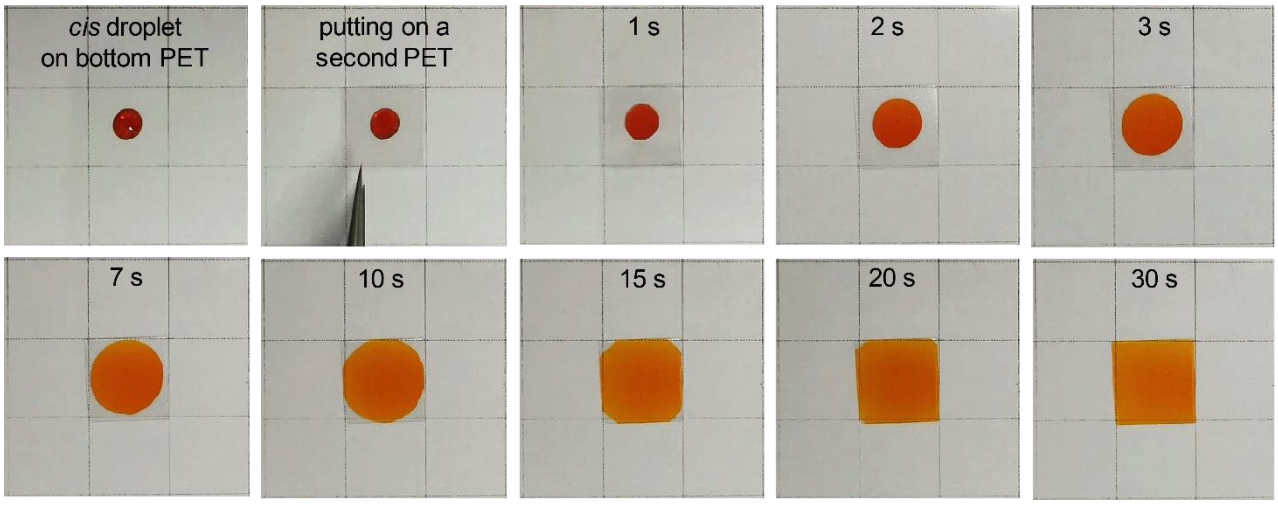

Figure S5. Photographs showing formation process of a *cis* liquid film (side length 10 mm). Transparent materials including PET films and glass slides have been used to fabricate the film devices.

Photo-discharging of *cis*-B8 film

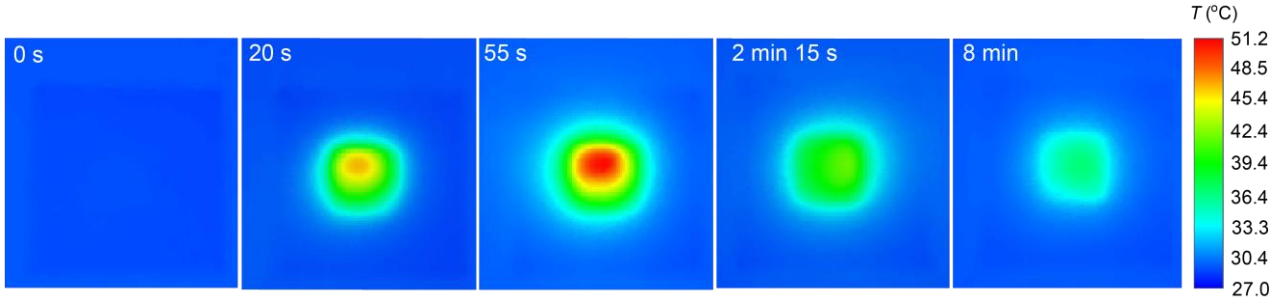

Figure S6. Representative IR thermal images during photo-discharging of a *cis*-**B8** film.

Supercooling property

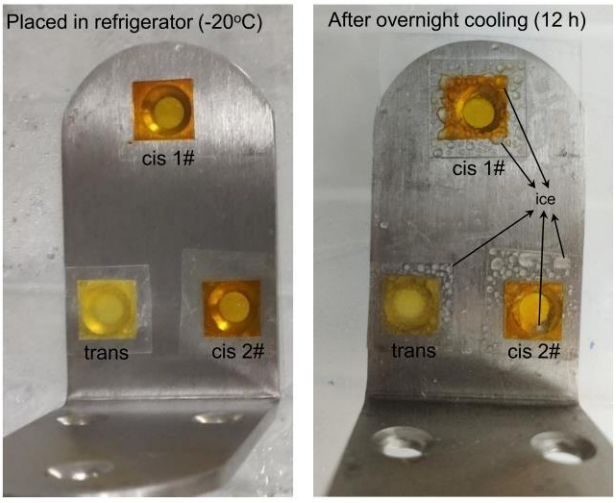

Figure S7. Photographs of films before and after stored in -20 °C refrigerator. The steel plate acts as a cold stage. Samples were adhered over the holes for convenience in examining their colour and transparency. After *cis*-B8 liquid (T_m = 19 °C) films were stored at -20 °C for 12 h, no sign of solidification was observed according to the colour and transparency. As a comparison, the water drops (T_m = 0 °C) on the film surface froze within 1 or 2 h in the refrigerator. Because of the high degree of supercooling, some of the *cis* samples (e.g., **A6**, **B6**, **B8**) in glass vials need to be stored in refrigerator for 1 or 2 days to get the *cis* solids.

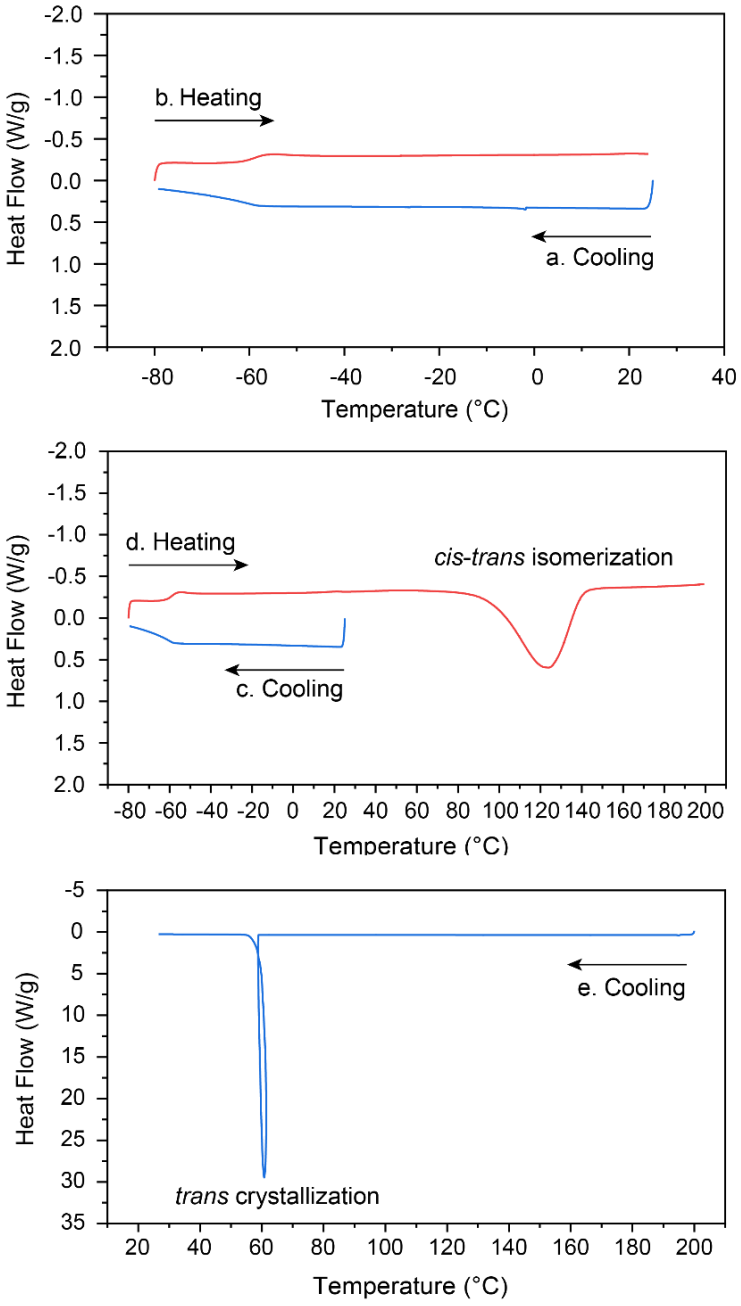

Figure S8. DSC curves of *cis*-B8 liquid (10 °C/min). The sample was programmed by: a. cooling from 25 to -80 °C; b. heating to 25 °C; c. cooling again to -80 °C; d. heating to 200 °C and e. cooling to 25 °C. In the cooling and heating cycles, crystallization of the *cis* liquid did not occur. Instead, the supercooled liquid state turned into glassy state with a glass transition temperature of -62 °C.

De-icing test

Figure S9. Experimental setup for de-icing tests.

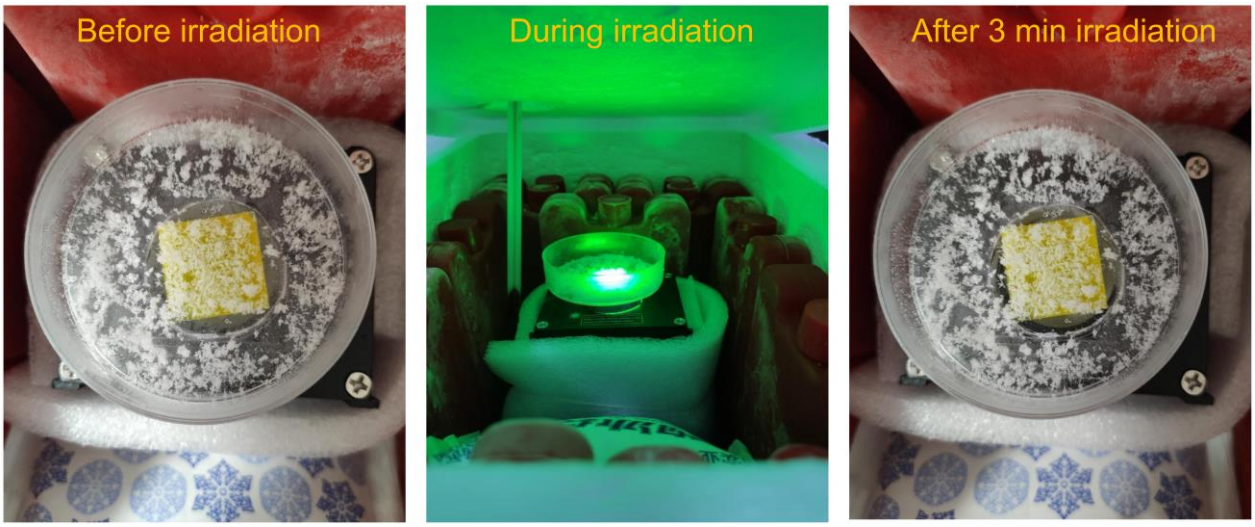

Figure S10. De-icing test using *trans*-**B8** solid film (blank experiment).

Reference

(1) Zhang, Z. Y.; He, Y.; Zhou, Y.; Yu, C.; Han, L.; Li, T. Pyrazolylazophenyl ether‐based photoswitches: facile synthesis, (near‐)quantitative photoconversion, long thermal half‐life, easy functionalization, and versatile applications in light‐responsive systems. *Chem. Eur. J.* **2019**, *25*, 13402-13410.

(2) Stranius, K.; Börjesson, K. Determining the photoisomerization quantum yield of photoswitchable molecules in solution and in the solid state. *Sci. Rep.* **2017**, *7*, 41145.

(3) Wang, Z.; Udmark, J.; Börjesson, K.; Rodrigues, R.; Roffey, A.; Abrahamsson, M.; Nielsen, M. B.; Moth-Poulsen, K. Evaluating dihydroazulene/vinylheptafulvene photoswitches for solar energy storage applications. *ChemSusChem* **2017**, *10*, 3049-3055.

(4) Kucharski, T. J.; Ferralis, N.; Kolpak, A. M.; Zheng, J. O.; Nocera, D. G.; Grossman, J. C. Templated assembly of photoswitches significantly increases the energy-storage capacity of solar thermal fuels. *Nat. Chem.* **2014**, *6*, 441-447.

(5) Luo, W.; Feng, Y.; Qin, C.; Li, M.; Li, S.; Cao, C.; Long, P.; Liu, E.; Hu, W.; Yoshino, K.; Feng, W. High-energy, stable and recycled molecular solar thermal storage materials using azo/graphene hybrids by optimizing hydrogen bonds. *Nanoscale* **2015**, *7*, 16214-16221.

(6) Jiang, Y.; Huang, J.; Feng, W.; Zhao, X.; Wang, T.; Li, C.; Luo, W. Molecular regulation of nano-structured solid-state azo-SWCNTs assembly film for the high-energy and short-term solar thermal storage. *Sol. Energy Mat. Sol. C.* **2019**, *193*, 198-205.

(7) Saydjari, A. K.; Weis, P.; Wu, S. Spanning the solar spectrum: azopolymer solar thermal fuels for simultaneous UV and visible light storage. *Adv. Energy Mater.* **2017**, *7*, 1601622.

(8) Wang, Z.; Losantos, R.; Sampedro, D.; Morikawa, M.; Börjesson, K.; Kimizuka, N.; Moth-Poulsen, K. Demonstration of an azobenzene derivative based solar thermal energy storage system. *J. Mater. Chem. A* **2019**, *7*, 15042-1504.